J. Mol. Biol. (1997) **270**, 99–110

JMB

Hydrogen Exchange in Chymotrypsin Inhibitor 2 Probed by Mutagenesis

José L. Neira, Laura S. Itzhaki, Daniel E. Otzen, Ben Davis and Alan R. Fersht*

MRC Unit for Protein Function and Design Cambridge Centre for Protein Engineering, University Chemical Laboratory Lensfield Road, Cambridge CB2 1EW, UK

**Corresponding author*

Two-dimensional NMR spectroscopy has been used to monitor hydrogen-deuterium exchange in chymotrypsin inhibitor 2. Application of two independent tests has shown that at pH 5.3 to 6.8 and 33 to 37°C, exchange occurs *via* an EX2 limit. Comparison of the exchange rates of a number of mutants of CI2 with those of wild-type identifies the pathway of exchange, whether by local breathing, global unfolding or a mixture of the two pathways. For a large number of residues, the exchange rates were unaffected by mutations which destabilised the protein by up to 1.9 kcal mol^{-1}, indicating that exchange is occurring through local fluctuations of the native state. A small number of residues were found for which the mutations had the same effect on the rate constants for exchange as on the equilibrium constant for unfolding, indicating that these residues exchange by global unfolding. These are residues that have the slowest exchange rates in the wild-type protein. We see no correspondence between these residues and residues involved in the nucleation site for the folding reaction identified by protein engineering studies. Rather, the exchange behaviour of CI2 is determined by the native structure: the most protected amide protons are located in regions of hydrogen bonding, specifically the C terminus of the α-helix and the centre of the β-sheet. A number of the most slowly exchanging residues are in the hydrophobic core of the protein.

Keywords: chymotrypsin inhibitor 2; NMR; nucleation; protein folding

Introduction

Backbone and side-chain NH groups of proteins are labile and exchange with solvent protons. The measurement of this exchange phenomenon has become an important tool in the study of structure, stability, folding, dynamics and intermolecular interactions in protein systems in solution (see, for the most recent review, Englander *et al.*, 1996). The key development has been the use of two-dimensional proton NMR spectroscopy to measure the rates of exchange of individual protons (Wüthrich, 1986). In contrast to the rapid progress in experimental measurement of $^{1}H/^{2}H$-exchange in proteins, the details of the mechanism of exchange and quantitative correlation with structure and internal mobility are still not fully understood (Woodward & Hilton, 1980; Englander & Kallenbach, 1984). Nevertheless, the various models agree upon a general two-process model (Woodward & Hilton, 1980; Bai *et al.*, 1994; Qian *et al.*, 1994). According to this model, there are two pathways for exchange: (1) global unfolding followed by exchange from the unstructured state ensemble of the protein, and (2) exchange from the native state ensemble by local fluctuations. The structural nature of these local fluctuations is particularly poorly understood. The premises of this model and the relationship between the model and

Present addresses: D. E. Otzen, Enzyme Function, Novo Nordisk A/S, Novo Alle, DK-2880 Bagsvaerd, Denmark; B. Davis, Ludwig Institute for Cancer Research, University College/Middlesex Hospital Branch, 91 Riding House Street, London WC1P 88T.

Abbreviations used: BPTI, basic pancreatic trypsin inhibitor; CI2, chymotrypsin inhibitor 2; GdmCl, guanidinium chloride; [GdmCl], concentration of guanidinium chloride; HSQC, heteronuclear single quantum coherence spectroscopy; NMR, nuclear magnetic resonance; 2D, two-dimensional; NOE, nuclear Overhauser effect; NOESY, two-dimensional nuclear Overhauser effect spectroscopy; PDLA, poly-D-L-alanine; TPPI, time proportional phase increment; TSP, [2,2,3,3-$^{2}H_4$]-(trimethylsilyl)propionate.

0022–2836/97/260099–12 $25.00/0/mb971088

the folding pathway of proteins can be verified in small single domain proteins, where tertiary structural factors from different domains are avoided. Further, analysis can be simplified by using a protein which conforms to two-state folding under both equilibrium and kinetic conditions, i.e. in which no intermediate, partially folded states are populated.

Truncated CI2 is a small, monomeric protein of 64 residues and consists of a single module of structure. It folds by simple two-state kinetics (Jackson & Fersht, 1991) with concurrent formation of secondary and tertiary structure (Otzen *et al*., 1994; Itzhaki *et al*., 1995). The only well-developed region of structure in the transition state for folding is the N-terminal of the α-helix and some distant residues in the sequence with which it makes contacts (Jackson *et al*., 1993b; Otzen *et al*., 1994; Itzhaki *et al*., 1995). A nucleation-condensation model has been invoked which involves the concomitant formation of a diffuse nucleus of interactions (consisting of the N-terminal residues of the α-helix, stabilised by long range interactions) and the condensation of structure around the nucleus as it is formed (Fersht, 1995). CI2 is the simplest system for folding studies and may be a model for individual domains of larger proteins (Otzen *et al*., 1994). In our studies we have used a truncated form of CI2 lacking the first 20 unstructured residues, where residue 1 corresponds to residue 20 of the long form. Crystallographic (McPhalen & James, 1987; Harpaz *et al*., 1994) and NMR (Clore *et al*., 1987a.b; Ludvigsen *et al*., 1991) studies have defined the secondary structure of CI2 as follows: residues Thr3 to Trp5, β-strand 1; Trp5 to Leu8, type III reverse turn; Leu8 to Gly10, type II reverse turn; residues Lys11 to Ser12, β-strand 2; residues Ser12 to Lys24, α-helix; residues Pro25 to Gln28, type I reverse turn; Gln28 to Val34 β-strand 3; Gly35 to Asp45 reactive site loop (extended structure); residues Arg46 to Asp52, β-strand 4; residues Asp52 to Asp55, turn; residues Asp55 to Ala58, β-strand 5 and residues Val60 to Gly64, β-strand 6.

Theoretical background

According to the Linderstrøm-Lang model (Linderstrøm-Lang, 1955), the exchange reaction of a protected amide only takes place after that proton is exposed to solvent as a result of a structural fluctuation. Once in contact with solvent, exchange occurs at the rate of an amide proton in an unstructured polypeptide. This is illustrated in the following scheme in which exchange occurs from an ''open'' state (an exchange-competent form of the protein), but not from the ''closed'' form (an exchange-incompetent form of the protein):

$$closed \underset{k_{cl}}{\overset{k_{op}}{\rightleftharpoons}} open \xrightarrow{k_{int}} exchange \qquad (1)$$

where k_{op} and k_{cl} are the rate constants for the opening and closing processes, respectively. Values of k_{int}, the intrinsic rate constant of exchange for the competent amide, are dependent on pH and local sequence and have been calculated using short, unstructured peptides (Bai *et al*., 1993).

The observed rate constant for the overall process shown in equation (1), k_{ex}, is given by the following equation (Lowry & John, 1910):

$$k_{ex} = 0.5\Big[(k_{op} + k_{cl} + k_{int}) - \sqrt{(k_{op} + k_{cl} + k_{int})^2 - 4k_{op}k_{int}}\Big] \qquad (2)$$

There are two limits for exchange (Hvidt & Nielsen, 1966). In the limit where $k_{cl} \gg k_{int}$ (the most common, ''EX2'', limit), chemical exchange is the rate-limiting step and equation (2) reduces to:

$$k_{ex} = \frac{k_{op}}{k_{cl}} k_{int} = K_{op} k_{int} \qquad (3)$$

where K_{op} is defined as the equilibrium constant for the conformational transition between the open and closed states. In the other limiting case, $k_{cl} \ll k_{int}$ (the ''EX1'' limit), each opening fluctuation leads to exchange and equation (2) simplifies to:

$$k_{ex} = k_{op} \qquad (4)$$

Under EX2 conditions, therefore, the exchange kinetics can be used to study the equilibrium between the open and closed states, provided that reliable values of k_{int} are available:

$$\Delta G_{ex} = -RT \ln K_{op} = -RT \ln\left(\frac{k_{ex}}{k_{int}}\right) \qquad (5)$$

where ΔG_{ex} is the free energy for the opening process, R is the gas constant and T is the temperature. In some cases, for example for a wild-type and a mutant protein, the intrinsic rate of exchange should be the same for both proteins except around the site of mutation, and hence the difference in the free energy of exchange is simply given by (Clarke *et al*., 1993; Perrett *et al*., 1995):

$$\Delta\Delta G_{ex} = -RT \ln\left(\frac{k_{ex}^{wt}}{k_{ex}^{m}}\right) \qquad (6)$$

where k_{ex}^{wt} and k_{ex}^{m} are the observed exchange rates for the wild-type protein and the mutant, respectively. Hence, the difference in free energy of exchange is calculated directly from the measured exchange rates, and does not rely on k_{int}.

By calculating the values of $\Delta\Delta G_{ex}$ of the two protein species using equation (6) and comparing them with the difference in the free energy of unfolding, $\Delta\Delta G_{U\text{-}F}$, obtained by chemical denaturation experiments at equilibrium, it is possible to determine which protons exchange by global unfolding ($\Delta\Delta G_{ex} = \Delta\Delta G_{U\text{-}F}$), which by a local fluctuation of the native state ($\Delta\Delta G_{ex} = 0$), and which by a mixture of the two pathways

($0 < \Delta\Delta G_{ex} < \Delta\Delta G_{U\text{-}F}$) (Clarke *et al.*, 1993; Perrett *et al.*, 1995).

Here, the exchange behaviour of wild-type CI2 and a number of its point mutations has been studied. We have carried out a two-part strategy: Firstly, we have investigated whether hydrogen exchange in CI2 can be approximated to the EX2 limit by two independent methods: by measuring the pH-dependence of the exchange rates of each proton, and by determining whether or not exchange for neighbouring protons is coupled (Wagner, 1980). Once an EX2 limit has been established, it is possible to look for structural correlations with the observed exchange rates. And secondly, we have determined values of $\Delta\Delta G_{ex}$, the change in the free energy of exchange upon mutation, for individual protons of a number of mutant proteins of CI2 relative to the wild-type protein. We can assign a global or local exchange pathway to each proton by comparing the values of $\Delta\Delta G_{ex}$ with $\Delta\Delta G_{U\text{-}F}$, the change in free energy of unfolding of the mutant proteins relative to wild-type.

Results

Measurements were made at a range of values of pH and temperature for wild-type and for three mutants of CI2 (Table 1). For reliable interpretation of the data, we have carried out equilibrium denaturation experiments and folding and unfolding kinetics in the same buffer used in exchange experiments (50 mM acetate, pH 5.3. ^2H_2O†).

Examples of the decay curves are shown in Figure 1. Exchange rate constants for wild-type CI2 at 33°C at three values of pH are given in Table 2 and for three mutants proteins at 37°C in Table 3. Cross-peaks for the protons of 38 of the possible 59 residues are observed and well-resolved in the first spectrum acquired after solution in the exchange buffer at pH 5.3 and 33°C. The majority of peaks disappeared within hours to days but some of them could be observed for up to two months. Most of the peaks that were not observed in the first spectrum are those of surface residues or residues at the edges of the β-strands, which exchange too rapidly to measure under our conditions. The cross-peaks of residues Glu15, Asp23 and Leu54 could not be measured accurately because of their intrinsically small coupling constants. Residues Asp55 and Asn56, and residues Lys24 and Leu49, respectively, overlap under some of the conditions used. In these cases, the decay of intensity was fitted to a double exponential in order to obtain values of k_{ex} for both amide protons. The values of ΔG_{ex} calculated using the intrinsic rate constants from model peptide studies (Bai *et al.*, 1993; equation (3)), and assuming exchange occurs in the EX2 limit (see Discussion), are shown in Figure 2 for wild-type at the three values of pH.

† pH quoted is the pH read from the pH meter.

Table 1. Experimental conditions used for hydrogen exchange measurements in CI2

Protein	Temperature (°C)	pH
Wild-type	33	5.3, 5.7, 6.8
	37	6.3
Ile20Val	37	6.3
Ser12Gly/Glu14Ala/Glu15Ala	37	6.5
Ala58Gly	37	6.0

Comparison of the free energy of exchange with the free energy of unfolding

GdmCl-induced equilibrium denaturation experiments were performed in the exchange buffer (50 mM acetate, pH 5.3, ^2H_2O) at 33°C, and monitored by fluorescence (Figure 3). The midpoint of unfolding, $[GdmCl]_{50\%}$, which can be measured reproducibly for CI2 using fluorescence detection, is 3.7(±0.01) M, which is the same, within error, as the measured in water at the same pH and temperature. The *m*-value, which is the slope of the plot of $\Delta G_{U\text{-}F}$ *versus* [GdmCl], in ^2H_2O (1.9(±0.03) kcal mol^{-1} M^{-1}) is also close to that measured in water. The value obtained for $\Delta G_{U\text{-}F}$ is 7.0(±0.02) kcal mol^{-1}.

For the majority of protons, ΔG_{ex} is smaller than $\Delta G_{U\text{-}F}$ as determined by fluorescence (Table 2 and Figure 2), indicating that these protons exchange from the native-state ensemble under the conditions used. For a small number of protons, shown in bold in Table 2, the exchange rates were very slow at 33°C and, for some, accurate values could be determined only at the highest pH of 6.8 (even at pH 5.7 the exchange was too slow to provide an accurate measurement). We can estimate an average value of ΔG_{ex} for these protons ≈7.6(±0.3) kcal mol^{-1}. $^1H/^2H$-exchange measurements were also made at 37°C for the mutant studies (see below), and the slowest exchange rates were observed for the same group of protons, with measurable rates giving an average value of ΔG_{ex}

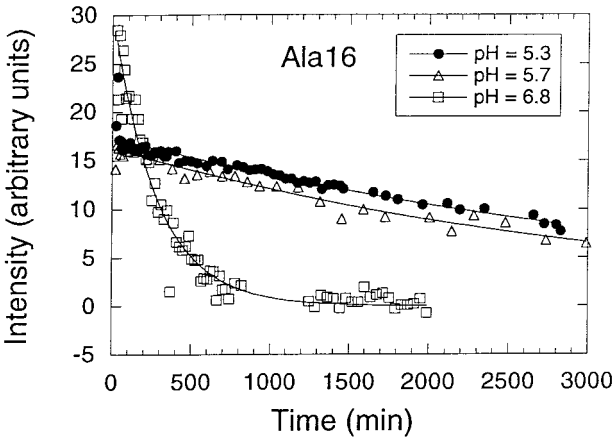

Figure 1. Hydrogen exchange behaviour for Ala16 in wild-type CI2 at 33°C and three values of pH (circles, pH 5.3; triangles pH 5.7 and squares pH 6.8).

Table 2. Rate constants for exchange (k_{ex}, min^{-1}) and free energies for exchange for wild-type CI2, measured at 33°C[a,b]

Residue[b]	$k_{ex}/10^{-4}$ pH 5.3	ΔG_{ex}[d] (kcal mol^{-1})	$k_{ex}/10^{-4}$ pH 5.7	ΔG_{ex}[d] (kcal mol^{-1})	$k_{ex}/10^{-4}$ pH 6.8	ΔG_{ex}[d] (kcal mol^{-1})
Glu4[e]	615	2.4	1665	2.3		
Trp5	3.4	5.2	2.3	5.9	36	5.8
Leu8	3.0	5.0	3.8	5.4	41	5.5
Val9	6.3	4.3	10.8	4.5	83	4.8
Gly10[e]	75	4.3	123	4.5		
Lys11[c]	<0.1		0.6	7.8	7.2	7.8
Val13	25	4.2	32	4.6	1490	3.8
Glu15[e]	917	1.7	2527	1.5		
Ala16	3.0	5.8	3.0	6.4	36	6.4
Lys17[e]	135	3.7	236	3.8		
Lys18	32	4.7	53	4.9	1100	4.6
Val19	1.4	5.6	2.7	5.8	27	6.0
Ile20[c]	<0.1		<0.1		<0.1	
Leu21[c]	<0.1		<0.1		2.5	7.1
Gln22	2.5	6.0	3.0	6.4	37	6.4
Asp23[e]	329	3.1	474	3.4		
Lys24	2.3	5.9	3.3	6.2	21	6.6
Ala27	37	4.3	52	4.6	380	4.9
Gln28	15	5.2	33	5.2	283	5.4
Ile30[c]	<0.1		0.3	6.7	1.0	7.4
Leu32[c]	<0.1		0.9	6.3	5.1	6.8
Val34	69	2.8	158	2.8		
Arg46	2.7	6.0	3.3	6.4	31	6.6
Val47[c]	<0.1		<0.1		<0.1	
Arg48	0.8	6.8	3.4	6.4	25	6.8
Leu49[c]	<0.1		<0.1		1.3	8.1
Phe50[c]	<0.1		<0.1		3.3	7.4
Val51[c]	<0.1		<0.1		<0.1	
Asp52	6.0	5.0	10.6	5.2	64	5.6
Leu54	551	2.3				
Asp55[e]	318	2.5	1230	2.2		
Asn56[e]			19	5.8	39	7.0
Ile57	1.1	6.1	0	6.7	18	6.4
Ala58	9.7	5.0	33	4.8	213	5.2
Gln59	4.4	5.9	11.6	5.8	61	6.4
Arg62	1.2	6.4	2.5	6.5	21	6.7
Val63	6.2	4.9	9.6	5.2	73	5.5
Gly64	2.1	3.6	1.7	4.2	13	4.5

[a] Errors in the determination of k_{ex} are of the order of 10 to 20%.
[b] Residues indicated in bold are those which exchange by a global unfolding pathway.
[c] Residues for which exchange rates were too slow to be measured accurately at the lower values of pH.
[d] ΔG_{ex} was determined using equation (5).
[e] Overlap or very rapid exchange precluded measurement of an accurate k_{ex} at certain values of pH.

of 7.8(±0.4) kcal mol^{-1} for wild-type (data not shown).

In conclusion, the most slowly exchanging protons are those of residues Lys11, Ile20, Leu21, Ile30, Val47, Leu49, Phe50 and Val51. Exchange rates of amide protons in denatured CI2 have been measured at 40°C and pH 1.5 (Y.-J. Tan & A. R. F., unpublished results). The protection factors were close to 1, indicating that the intrinsic exchange rates of the model peptides provide a good estimate of the exchange rates from the unfolded state of CI2. The agreement between ΔG_{ex} and $\Delta G_{U\text{-}F}$ indicates, therefore, that these protons exchange by a global unfolding pathway and that the exchange-competent state is essentially unstructured. Some of these conclusions can be verified by comparative exchange studies on mutant proteins (see Discussion).

Comparison with previous $^1H/^2H$-exchange results for CI2

A qualitative analysis of CI2 exchange behaviour has been reported previously (Ludvigsen *et al.*, 1991). There is in general good agreement with our results: the slowest-exchanging protons identified here are the slowest in previous work also. There are, however, differences for residues at the edge of the β-strands: for example, the amide proton of Glu4 was reported to be fast in the former analysis (at pH 4.2 and 25°C, compared with our conditions of pH 5.3 and 33°C). A theoretical study also agrees qualitatively with our results (Li & Daggett, 1995).

A quantitative study at pH 4.2 and 298 K has been carried out for a small set of protons (Jandu *et al.*, 1990); the reported rate constants are higher

Table 3. Rate constants for exchange (k_{ex}, min^{-1}), protection factors (P)[a] and $\Delta\Delta G_{ex}$[b] values for three mutants of CI2, measured at 37°C

	Ile20Val pH 6.3			Ser12Gly/Glu14Ala/Glu 15Ala pH 6.5			Ala58Gly pH 6.0		
Residue	$k_{ex}/10^{-4}$	$P/10^3$	$\Delta\Delta G_{ex}$	$k_{ex}/10^{-4}$	$P/10^3$	$\Delta\Delta G_{ex}$	$k_{ex}/10^{-4}$	$P/10^3$	$\Delta\Delta G_{ex}$
Trp5	31.6	8.3	0.4	57.3	7.3	0.5	25.4	5.2	0.7
Leu8	30.7	5.8	0.0	41.1	6.8	−0.1	31.5	2.8	0.4
Val9	120	1.0	0.4	167	1.1	0.3	95.5	0.6	0.7
Lys11	26.4	49.0	0.8	90.0	22.0	1.3	30.7	21	1.4
Val13	180	2.1	−0.5	1030	0.7	0.3	383	0.5	0.4
Ala16	29.9	22.6	0.1	51.0	20.5	0.1	29.2	11.6	0.5
Lys17	[c]			1440	0.9	−0.1	886	0.5	0.3
Lys18	[c]			[c]			379	1.5	0.4
Val19	54.6	4.6	0.6	93.0	4.3	0.6	42.1	3	0.9
Ile20	4.7[d]	26.8	1.7	17.3	11.8	2.2	3.0	21.8	1.8
Leu21	8.7	16.4	1.2	24.9	9.4	1.6	9.1	8.1	1.7
Gln22	22.7	29.7	0.0	[c]			23.8	14.2	0.4
Lys24	22.9	25.2	0.2	48.8	18.7	0.4	20.5	14.1	0.6
Ala27	380	1.8	0.01	560	1.9	0.1	422	0.8	0.6
Gln28	180	6.2	0.1	405	4.3	0.4	263	2.1	0.8
Ile30	5.4	19.5	1.2	13.1	12.2	1.4	5.4	9.7	1.6
Leu32	9.7	18.8	0.3	14.3	20.2	0.2	14.8	6.2	1.0
Val34	240	0.75	0.6	[c]			228	0.2	1.0
Arg46	48.8	15.5	0.4	71.6	16.8	10.3	43.7	8.7	
Val47	7.3	43.3	1.3	16.9	29.8	1.5	8.0	19.8	1.8
Ag48	46.8	17.8	0.4	78.0	16.9	0.4	43.2	9.6	0.7
Leu49	[c]			48.8	13.5	1.4	[c]		
Phe50	17.5	19.4	1.1	28.5	18.8	1.1	[c]		
Val51	4.2	52.1	1.3	16.6	20.1	1.8	6.6	16.7	2.0
Asp52	50.8	6.8	−0.2	88.5	6.2	−0.1	[c]		
Asn56	70.0	27.8	0.1	118	26.2	0.1	148	6.6	1.0
Ile57	14.6	25.4	0.3	62.3	9.5	1.0	27.0	6.9	1.1
Ala58	170	3.3	−0.1	169	5.3	−0.4	[c]		
Gln59	100	10.8	0.1	172	10.1	0.2	[c]		
Arg62	44.0	15.0	0.5	63.1	16.6	0.4	31.6	10.5	0.7
Val63	90.9	3.5	0.1	142	3.5	0.1	86.3	1.8	0.5
Gly64	29.0	0.4	0.7	20.8	0.8	0.2	44.0	0.1	1.3

[a] Protection factor, $P = k_{int}/k_{ex}$.
[b] Calculated from equation (6) or (8) using wild-type data measured at the same temperature and at pH 6.3.
[c] Overlap or very rapid exchange precluded accurate measurement of exchange rates.
[d] Site of mutation.

than those described here. The discrepancies between both sets of results and those reported here probably result from the lower stability of CI2 at values of pH below 5 (Jackson *et al.*, 1993a,b; Tan *et al.*, 1995). Further, some acidic groups in CI2 titrate at pH 4.2 (Tan *et al.*, 1995) and so may affect the exchange rates, as has been shown for lysozyme (Delepierre *et al.*, 1987).

Discussion

EX2 *versus* EX1 limit

We have used two approaches to differentiate between EX2 and EX1 limits of exchange. In the EX2 limit the protein undergoes many opening reactions before one particular amide proton exchanges. The exchanges of neighbouring amide protons are not coupled whatever the nature of the opening fluctuations. In contrast, there is cooperativity of the exchange process in the EX1 limit (equation (4)) where the opening process is directly observed. Thus, correlated exchange for neighbouring residues is a sufficient criterion to distinguish between EX1 and EX2 limits, but it is not a necessary condition.

It can be shown (Wagner, 1980) that two amide protons, A and B, which are close in space, will exhibit uncoupled exchange under the EX2 limit, and, therefore, the intensity of the NOE between them will be the product of the individual intensities. Thus, the decay rate of the NOE signal, k_{ex}^{AB}, will be:

$$k_{ex}^{AB} = k_{ex}^{A} + k_{ex}^{B},$$

where k_{ex}^{A} and k_{ex}^{B} are the rates observed for protons A and B, respectively. On the other hand, in the EX1 limit, A and B exchange will occur at the same rate and the rate of the observed NOE between them will be:

$$k_{ex}^{AB} = k_{ex}^{A} = k_{ex}^{B}.$$

This approach has been applied successfully to BPTI (Wagner, 1980; Roder *et al.*, 1985); cytochrome *c* (Bai *et al.*, 1994) and ovomucoid third domain (Swint-Kruise & Robertson, 1996).

The second method for distinguishing between EX1 and EX2 is based on the principle that under

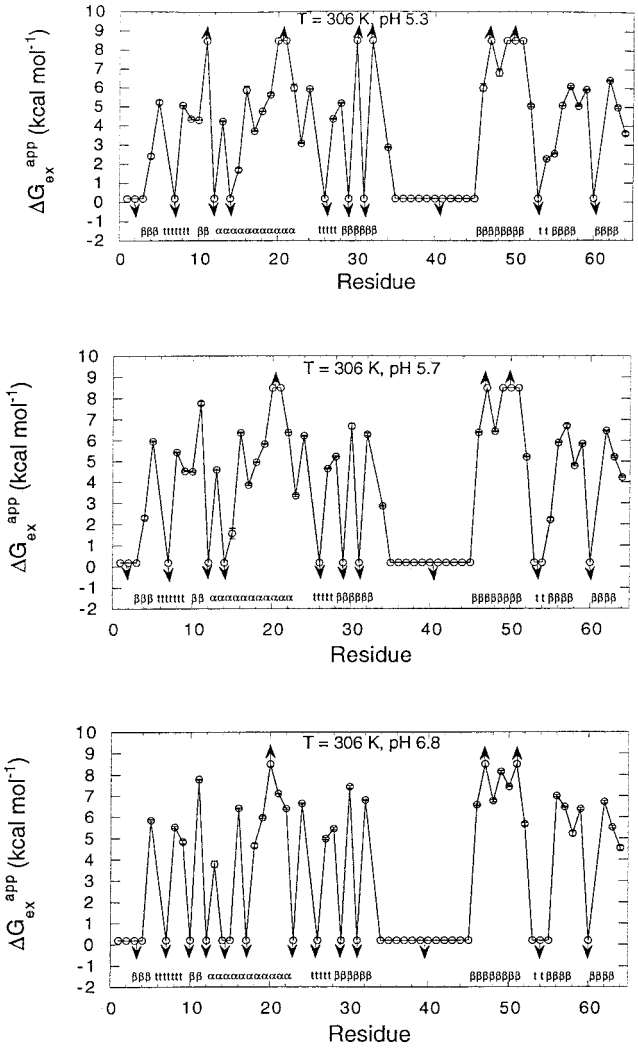

Figure 2. ΔG_{ex} for wild-type CI2 at 33°C and three different pH values. The secondary structure is indicated using α for an α-helix, β for a β-sheet and t for turn (Ludvigsen *et al.*, 1991). Upward and downward-pointing arrow indicate residues whose exchange was too slow and too fast, respectively, to measure.

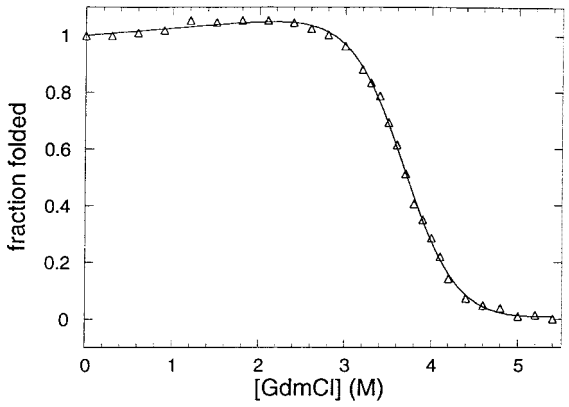

Figure 3. Equilibrium GdmCl-induced denaturation in exchange buffer, ^2H_2O, pH 5.3, at 33°C, followed by fluorescence (excitation at 280 nm, emission at 356 nm). Continuous curve is the theoretical fit to the equation:

$$F = \{(\alpha_N + \beta_N \mathrm{GdmCl}]) + [\alpha_D \times \exp[m([\mathrm{GdmCl}] - [\mathrm{GdmCl}]_{50\%})/RT]\}/\{1 + \exp[m([\mathrm{GdmCl}] - [\mathrm{GdmCl}]_{50\%})/RT]\},$$

where F is the observed fluorescence, α_N and α_D are the intercepts of the baselines at the low (N) and high (D) GdmCl concentrations, and β_N is the slope of the baseline at the low GdmCl concentration. $[\mathrm{GdmCl}]_{50\%}$ is the concentration of GdmCl at which 50% of the protein is denatured. The free energy for unfolding is then calculated as:

$$\Delta G_{D-N}^{H_2O} = m[\mathrm{GdmCl}]_{50\%}.$$

EX1 conditions (equation (4)) there need be no pH-dependence of the observed exchange rate, whereas in the EX2 limit (equation (3)), k_{ex} will be proportional to the concentration of H_3O^+ or OH^- in the acid or base-catalysed reaction. Thus, in the base-catalysed region, a straight line with a slope of one in a plot of $\log k_{ex}$ against pH is diagnostic of EX2. A slope of zero indicates EX1. A plot of $\log k_{ex}$ for individual residues at one value of pH against those at another pH can also be used, with a slope of one indicating EX2, and a slope of zero indicating EX1 (Skelton *et al.*, 1992; Perrett *et al.*, 1995; Clarke & Fersht, 1996). This method fails if k_{op} has a similar pH-dependence to k_{int}, or if there are residues which titrate in the explored pH range. The two methods together provide good diagnostic evidence for a particular limit.

The first test was applied to CI2 at pH 5.3 and 33°C. Only a few sequential NH/NH NOEs and one medium-range NOE could be measured accurately (Table 4). Although the data are limited by low intensities of the NOEs, they are sufficient to show that there is an uncorrelated limit in all the pairs of protons examined, except for the NOEs corresponding to Ala58-Gln59 and Lys17-Lys18. For the latter residues, the data are not good enough to indicate whether there is correlated or uncorrelated exchange.

The second test of exchange limit was carried out at 33°C in the range of pH between 5.3 and 7.0. A plot of k_{ex} at pH 5.3 *versus* k_{ex} at pH 6.8 is shown in Figure 4. The slope of the plot is close to 1, indicating an EX2 limit.

The tests could not be applied to all of the global exchanging protons because the exchange rates were too slow to be measured accurately. However, exchange rates could be estimated or measured at the two higher values of pH for five out of the eight residues, and these exhibited, on average, a pH dependence that is expected for EX2 behaviour. Further, in the accompanying paper (Itzhaki *et al.*, 1997) the exchange rates were measured in increasing concentrations of the denaturant GdmCl, and an EX2 limit was observed at 33°C in 1.5 M GdmCl between pH 5.3 and 6.0, for all residues, including those that exchange by

Table 4. Determination of EX2 *versus* EX1[a]

Residue	k_{ex}^{A} or k_{ex}^{B} (min^{-1})[b]	$k_{ex}^{A} + k_{ex}^{B}$ (min^{-1})	k_{ex}^{AB} (min^{-1})[c]	Exchange limit
Leu8	$(30.3 \pm 0.9) \times 10^{-5}$	$(93 \pm 7) \times 10^{-5}$	$(12.9 \pm 4) \times 10^{-4}$	EX2
Val9	$(62.7 \pm 6) \times 10^{-5}$			
Gly10	$(7.5 \pm 0.3) \times 10^{-3}$	$(7.5 \pm 0.3) \times 10^{-3}$	$(5.4 \pm 1.4) \times 10^{-3}$	EX2
Lys11[d]	$<1 \times 10^{-6}$			
Lys17	$(13.5 \pm 0.3) \times 10^{-3}$	$(16.7 \pm 0.3) \times 10^{-3}$	$(5.1 \pm 2.2) \times 10^{-3}$	[e]
Lys18	$(32.2 \pm 0.6) \times 10^{-4}$			
Lys18	$(32.2 \pm 0.6) \times 10^{-4}$	$(33.6 \pm 0.6) \times 10^{-4}$	$(5.3 \pm 1) \times 10^{-4}$	EX2
Val19[d]	$(1.4 \pm 0.06) \times 10^{-4}$			
Leu21[d]	$<1 \times 10^{-6}$	$(2.4 \pm 0.7) \times 10^{-4}$	$(2.2 \pm 0.6) \times 10^{-4}$	EX2
Gln22	$(2.4 \pm 0.7) \times 10^{-4}$			
Ala58	$(9.7 \pm 0.6) \times 10^{-4}$	$(14.1 \pm 0.7) \times 10^{-4}$	$(2.8 \pm 0.2) \times 10^{-3}$	[e]
Gln59	$(4.4 \pm 0.1) \times 10^{-4}$			
Asp52	$(6.0 \pm 0.5) \times 10^{-4}$	$(3.8 \pm 0.2) \times 10^{-3}$	$(4.5 \pm 0.8) \times 10^{-3}$	EX2
Asn56	$(3.2 \pm 0.1) \times 10^{-3}$			

[a] Measurements were made at pH 5.3, 33°C, acetate buffer.
[b] Observed rates for peaks A and B, respectively, from ^{1}H-^{15}N HSQC experiments. The standard errors from fitting are indicated.
[c] k_{ex}^{AB} was determined from the decay of the NH/NH NOEs signals in the NOESY experiments. The standard errors from fitting are indicated.
[d] Residues for which accurate exchange rates could not be measured.
[e] The errors in the rate constants are too large to assign the $^{1}H/^{2}H$ limit.

global unfolding. If the limit of the globally exchanging residues is EX2 under conditions where the protein is significantly destabilised and the rate of the refolding is smaller, then it can be assumed that it is also EX2 under the more stabilising conditions in the absence of denaturant used here.

To conclude, both approaches indicate that the limit of exchange is EX2. Therefore, equation (3) can be used in the following studies, and thus the exchange rates can be converted to Gibbs free energies for the equilibrium between open and closed forms of the protein.

Relationship between hydrogen exchange and structure

The hydrogen bond scaffold of wild-type CI2 (Ludvigsen *et al.*, 1991) is shown in Figure 5. Protection against exchange of amide protons in proteins has been attributed to intramolecular hydrogen bonding or burial from solvent (Englander & Kallenbach, 1984). In CI2, all the amide protons whose exchange rates were slow enough to be measured are hydrogen bonded, with the exception of those of Glu4, Glu15, Phe50, Leu54 and Arg62† (McPhalen & James, 1987; Ludvigsen *et al.*, 1991), and are located either in the β-sheet or in the unique α-helix, indicating that there is reduced structural fluctuation in these regions. Residues that are not protected from exchange are located in regions of irregular structure. The protected amide protons all have zero solvent-exposed surface area, as determined by the method of Lee & Richards (1971) (Figure 6). However, this does not appear to be a sufficient condition for

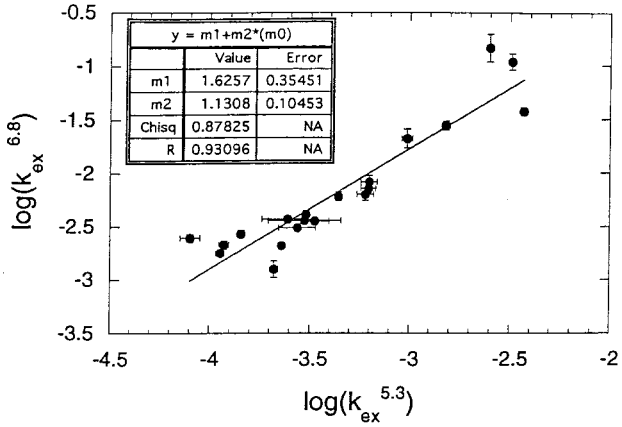

Figure 4. Plot of exchange rates at 33°C at two values of pHs. The value of log k_{ex} at pH 5.3 is plotted against the value of log k_{ex} at pH 6.8 for the same residue. Error bars from fitting are shown.

† Arg62 is involved in hydrogen bonding bridges with water (Ludvigsen *et al.*, 1991; Li & Daggett, 1995); thus, it may be partially protected from exchange with bulk water.

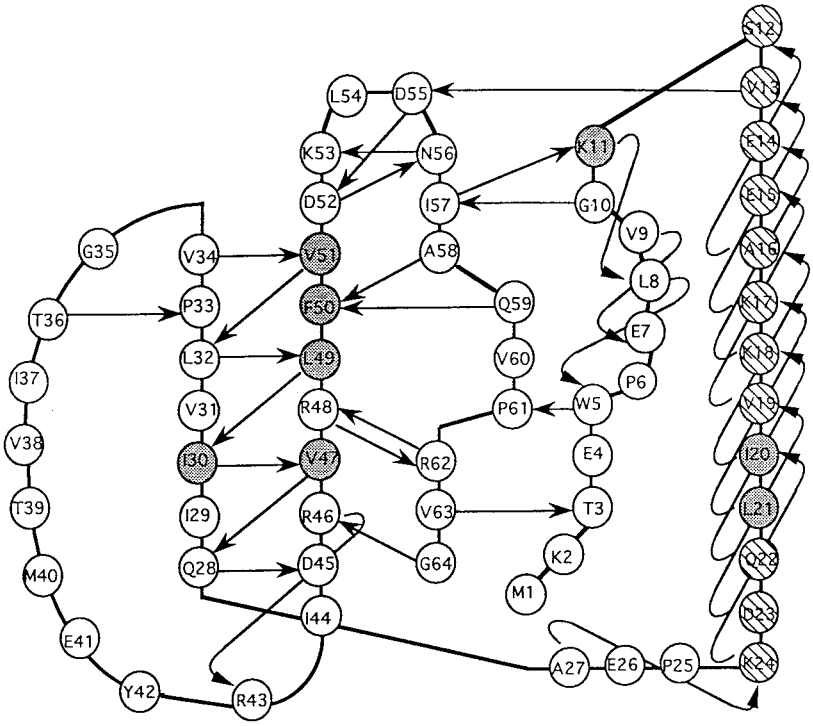

Figure 5. Schematic representation of the hydrogen-bond scaffold of wild-type CI2 (Ludvigsen *et al.*, 1991) showing residues forming the protein folding core (hatched circles) (Itzhaki *et al.*, 1995) and residues which exchange by a global unfolding mechanism (filled circles).

slow exchange, since some of the fast-exchanging protons, for example that of Glu7, are also completely buried from solvent.

CI2 has a unique α-helix which packs against the β-sheet to form the hydrophobic core of the protein. The other side of the helix is exposed to solvent. There is a qualitative correlation between the calculated ΔG_{ex} and the distance of the amide protons to the surface of the protein: residues Ile20 and Leu21 interact with the β-sheet to form the hydrophobic core and are the most buried in the helix. These have the highest values of ΔG_{ex}. Residues Ala16 and Lys24 are partially buried and have intermediate values of ΔG_{ex}.

The most protected strands of the β-sheet are the central strands, 3 and 4. Residues in these strands pack against the α-helix in the core of the protein, and exchange by global unfolding. The rest of the β-sheet is exposed to the solvent by local fluctuations.

To summarise, the slowest exchanging protons are located in the C-terminal of the α-helix and central strands of the β-sheet. They belong to the hydrophobic core, but they are not involved in the folding core, which is formed by the N-terminal residues of the α-helix (Otzen *et al.*, 194; Itzhaki *et al.*, 1995).

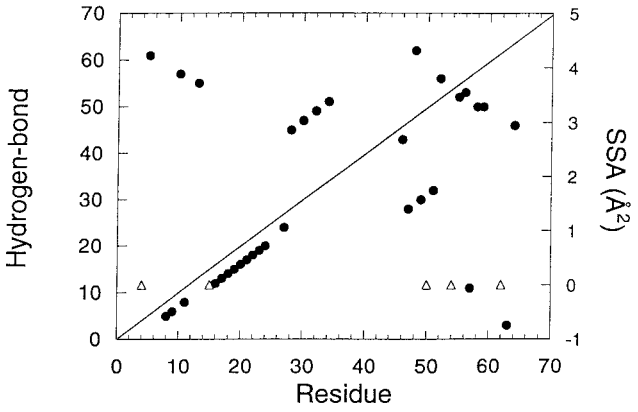

Figure 6. Examination of the structural basis for retardation of hydrogen exchange. The axes represent the 64 amino acid residues in CI2. Filled circles indicate slowly-exchanging amide protons with zero solvent-accessibility, and their hydrogen-bonding partner (left axis). Triangles indicate those slowly-exchanging residues with zero solvent-accessibility (SSA right axis; Lee & Richards, 1971) which are not hydrogen-bonded.

Global *versus* local exchange

Comparison of the exchange behaviour of wild-type and mutant proteins allows us to determine the pathway of exchange, whether by local fluctuations, global unfolding or a mixture of the two. It is a particularly valuable approach, because it requires neither knowledge of the intrinsic rate constants nor a good estimate for $\Delta G_{U\text{-}F}$ (equation (6)). These are both needed in order to distinguish the pathway of exchange from wild-type data alone (see above). Only the value of $\Delta\Delta G_{U\text{-}F}$ for mutant relative to wild-type is required and this can be determined with much greater certainty than can $\Delta G_{U\text{-}F}$. We have measured the exchange behaviour of three mutants of CI2 which destabilise the protein by 1.3 to 1.9 kcal mol^{-1} (Jackson *et al.*, 1993a; elMasry & Fersht, 194; Itzhaki *et al.*, 1995). The mutants are Ile20Val ($\Delta\Delta G_{U\text{-}F} = 1.30$ kcal mol^{-1}), Ser12Gly/Glu14Ala/Glu15Ala ($\Delta\Delta G_{U\text{-}F} = 1.63$ kcal mol^{-1}), and Ala58Gly ($\Delta\Delta G_{U\text{-}F} = 1.88$ kcal mol^{-1}). In general, the exchange rates (Table 3) reflect the

Table 5. Ratio of $\Delta\Delta G_{ex}/\Delta\Delta G_{U\text{-}F}$ for mutants of CI2[a]

Residue	Ile20Val	$\Delta\Delta G_{ex}/\Delta\Delta G_{U\text{-}F}$ Ser12Gly/Glu14Ala/ Glu15Ala	Ala58Gly
5	0.3	0.3	0.4
8	0.0	−0.1	0.2
9	0.3	0.2	0.3
11	**0.6**	**0.8**	**0.7**
13	−0.4	0.2	0.2
16	0.1	0.1	0.3
17	[b]	−0.1	0.2
18	[b]	[b]	0.2
19	0.5	0.4	0.5
20	**1.3**[c]	**1.3**	**1.0**
21	**1.0**	**1.0**	**0.9**
22	0.0	[b]	0.2
24	0.2	0.3	0.3
27	0.1	0.0	0.3
28	0.1	0.2	0.4
30	**0.9**	**0.9**	**0.9**
32	0.2	0.1	0.5
34	0.4	[b]	0.5
46	0.3	0.2	0.4
47	**1.0**	**0.9**	**0.9**
48	0.3	0.2	0.4
49	[b]	**0.9**	[b]
50	**0.8**	**0.7**	[b]
51	**1.0**	**1.1**	**1.1**
52	−0.1	−0.1	[b]
56	0.1	0.1	0.5
57	0.3	0.6	0.6
58	−0.1	−0.2	[b]
59	0.1	0.1	[b]
62	0.4	0.3	0.4
63	0.1	0.1	0.3
64	0.5	0.1	0.7

[a] $\Delta\Delta G_{ex}$ was calculated according to equation (6) or (8) using data shown in Table 3. Residues with $\Delta\Delta G_{ex}/\Delta\Delta G_{U\text{-}F}$ close to 1 are in bold. Those with $\Delta\Delta G_{ex}/\Delta\Delta G_{U\text{-}F}$ close to 0 are underlined.

[b] Overlap or very fast exchange precluded accurate measurement of exchange rate.

[c] Site of mutation.

stability of the protein. Values of $\Delta\Delta G_{ex}/\Delta\Delta G_{U\text{-}F}$ are given in Table 5. Residues for which $\Delta\Delta G_{ex}/\Delta\Delta G_{U\text{-}F}$ is close to 1 can be identified as globally exchanging and are shown in bold. Residues for which $\Delta\Delta G_{ex}/\Delta\Delta G_{U\text{-}F}$ is close to 0 can be identified as exchanging by local fluctuation and are underlined. The mean value of the free energies of the globally exchanging residues thus identified was determined for each mutant and is very close to the value obtained by equilibrium denaturation measurement (Jackson *et al.*, 1993a; Itzhaki *et al.*, 1995).

The same pattern of exchange is observed in all three mutants. The majority of residues exchange by local fluctuations. Eight residues, namely Lys11, Ile20, Leu21, Ile30, Val47, Leu49, Phe50 and Val51, appear to exchange by global unfolding. This confirms the conclusions reached from the analysis of the wild-type data, in which we assigned a global exchange pathway to all of these residues. Residues Ile20, Val47, Leu49 and Val51, are in the hydrophobic core. Residue Leu21, on the edge of the core, is in the last turn of the 13-residue α-helix. All the residues in the first two turns of the helix undergo local exchange. This includes residue Ala16 which is partially buried and in the folding core. The results indicate that there is no relationship between folding pathway and exchange pathway: the folding core or nucleus (Itzhaki *et al.*, 1995) consists of the N-terminal residues of the α-helix, including Ala16, and tertiary interactions of the side-chain of Ala16 with the side-chains of Leu49 and Ile57.

State from which the $^1H/^2H$-exchange takes place

Native structures of proteins are stabilised by free energies of only 5 to 15 kcal mol^{-1} relative to the unfolded state (Creighton, 1993). Under native conditions all possible states are accessible, even the fully unfolded state, but the relative populations, given by the Boltzmann distribution, depend on the free energy of each state. Folding studies of CI2 have shown that only two states are significantly populated under all conditions: the native-state ensemble and the unfolded-state ensemble (Jackson & Fersht, 1991). The protection factors for the slowest exchanging amide protons in the wild-type protein are close to the equilibrium constant for global unfolding obtained by fluorescence denaturation ($\Delta G_{ex} \approx \Delta G_{U\text{-}F}$), and mutation has the same effect on these protection factors as on the equilibrium constant for unfolding ($\Delta\Delta G_{ex} \approx \Delta\Delta G_{U\text{-}F}$). This indicates that these protons have the same structural fluctuation for exchange, namely global unfolding, that exchange occurs from the high-energy unfolded state ensemble, and that this state is likely to be essentially unstructured. Since the eight globally exchanging residues are reasonably well distributed throughout the sequence, it is likely that the entire polypeptide chain, and not just a small section, is unstructured. For the other, majority, of protons, $\Delta G_{ex} < \Delta G_{U\text{-}F}$ and $\Delta\Delta G_{ex} < \Delta G_{U\text{-}F}$, indicating that exchange occurs from the native-state ensemble.

Relationship between exchange and folding pathway of CI2

CI2 folds by simple two state kinetics, in which there are no intermediates and only a single, rate-determining transition state (Jackson & Fersht, 1991). A nucleation-condensation mechanism has been invoked for the folding reaction, in which the overall structure condenses around a nucleus, consisting of the unique α-helix stabilised by long range contacts (Fersht, 1995). The N-terminal region of the α-helix is the only element of structure which is well-developed in the transition state (Itzhaki *et al.*, 1995), and residue Ala16 makes its fully native interactions in the transition state with the side-chains of Leu49 and Ile57.

It has been proposed, based on BPTI results, that the protein folding core is within the slow-folding core, i.e. the slowest-exchanging protons (Kim *et al.*, 1993). This is not the case for barnase (Clarke *et al.*,

1993; Perrett *et al.*, 1995; Clarke & Fersht, 1996): some regions which are formed early in the folding reaction do not belong to the group of slowest-exchange protons of the enzyme, while tertiary interactions, known to be formed late during the folding pathway, involved some of the slowest-exchanging protons in barnase. The difference between the $^1H/^2H$-exchange and the folding pathway is also clear in CI2. The N-terminal of the α-helix, which is the folding nucleus for CI2, does not belong to the set of slowest-exchanging protons in CI2, mainly because some of those protons are partially solvent-exposed (Ser12, Val13 and Glu14). Further, ΔG_{ex} for Ala16 at pH 5.3 and 306 K is 5.8 kcal mol^{-1}, which is well below the global stability of the protein. In CI2 the slowest-exchanging region of the protein is the hydrophobic core, mainly because of the β-sheet scaffold and the reduced solvent-accessibility: in contrast the residues involved in the folding core are partially exposed and hence their exchange is rapid.

Materials and Methods

Materials

Deuterium oxide (99% atom in ^2H_2O) was obtained from Goss Scientific Instruments Ltd; TSP was obtained from Aldrich Chemical Co. (Gillingham, UK); d_3-acetic acid and d_3-sodium acetate were purchased from SIGMA. $^{15}NH_4Cl$ was from CK gas, UK. Standard suppliers were used for all other chemicals and water was deionized and purified on an Elgastat system.

The exchange buffer was 50 mM d_3-acetate. The pH of all samples was measured at the beginning and end of every experiment using a Russell glass electrode at the temperature of the experiment. No differences were found between pH measurements at the beginning and end of the experiments. Values of pH reported here for ^2H_2O solutions represent apparent values of pH, without correction for isotope effects.

Expression and purification of proteins

Wild-type and mutant CI2 were expressed and purified as described elsewhere in rich or minimal medium (Jackson *et al.*, 1993a). The mutants used were Ser12Gly/Glu14Ala/Glu15Ala, Ile20Val and Ala58Gly. The purified proteins were dialysed against several changes of deionized water and lyophilised.

GdmCl equilibrium denaturation experiments

GdmCl-induced equilibrium denaturation of wild-type CI2 was followed by fluorescence in the exchange buffer in ^2H_2O, at 33°C in 50 mM acetate buffer at pH 5.3. Fluorescence was monitored at an excitation wavelength of 280 nm and an emission wavelength of 356 nm. The experiment was repeated three times. For comparison, denaturation in H_2O under the same conditions of buffer, pH and temperature, was performed. A detailed description of the experimental procedure and data analysis has been published previously (Jackson *et al.*, 1993a, Itzhaki *et al.*, 1995).

NMR spectroscopy

The spectra were recorded on a Bruker AMX-500 spectrometer, equipped with a Haake temperature unit. The varying temperature of the spectrometer was equilibrated using a methanol standard solution (Van Greet, 1968). For each sample the temperature was calibrated immediately prior to data acquisition. The temperature used for the wild-type measurements was 33°C, and for the mutant studies 37°C. Shims were adjusted prior to the experiment on a sample similar to the exchange sample.

Exchange samples for NMR were prepared by dissolving a lyophilised aliquot from a stock solution of wild-type or mutant CI2 in 500 µl of pre-cooled exchange buffer. The solution was centrifuged briefly to remove insoluble protein and transferred to a 5 mm NMR tube. After transferring the sample tube to the spectrometer, the lock signal was monitored to determine temperature equilibration. Shims were readjusted and data acquisition was begun. The first spectrum was recorded approximately 10 to 15 minutes after the dissolution of the protein. ^1H and ^{15}N chemical shifts are quoted relative to external TSP and $(^{15}NH_4)_2SO_4$, respectively.

The exchange behaviour of CI2 wild-type and mutants was followed by the so-called tandem method (Wang *et al.*, 1995). 2D heteronuclear ^1H-^{15}N HSQC spectra (Bax *et al.*, 1990) were acquired with increasing delays for up to four days. Spectra were acquired with two, four or eight scans per increment depending on the sample. Typically, about 30 experiments were acquired within the first 24 hours. During data acquisition the carrier frequency of the NMR spectrometer was set on the water signal, and the spectral width was 4000 Hz in the ^1H dimension and 3000 Hz in the ^{15}N dimension. The spectra were recorded with 2048 complex data points, and 128 t_1 increments using the TPPI method (Marion & Wüthrich, 1983).

The NOESY-detected exchange experiment used to distinguish between EX2 and EX1 test was performed at pH 5.3, 33°C. Homonuclear NOESY spectra (Jeener *et al.*, 1979) were recorded on an unlabelled sample. Acquisition time was four hours and therefore the number of spectra that could be collected were limited to 12. The spectra were recorded with 2048 complex data points, and 256 t_1 increments (88 scans per experiment) using the TPPI method. The spectral width was set to 8064 Hz in both dimensions. The water signal was attenuated using presaturation during the relaxation delay (one second) and the mixing time (100 ms).

Processing was carried out using the Bruker UXNMR software, on a SGI workstation. Prior to Fourier transformation, the homo- and heteronuclear spectra were zero-filled to 2048 × 1024 data points. Mild gaussian window functions were used throughout all the HSQC experiments, and sine-bell squared (shifted $\pi/4$ in the t_2 dimension and $\pi/6$ in the t_1 dimension) for he NOESY experiments. Phase and base line corrections were applied in every case.

Assignment of ^1H-^{15}N HSQC experiments of wild-type and mutants was carried out by comparison of the observed chemical shifts with the reported assignments (Kjær *et al.*, 1987) and using our own data (B. D. & A. R. F., unpublished results). The volume integrals of the cross-peaks were calculated using the BRUKER program for each spectrum. Attempts to compensate for base plane differences between the spectra were made by subtracting values of peaks obtained in regions of noise, from cross-peak values. The results only diminished data

quality, and, thus, base plane differences have been ignored in rate determinations.

Hydrogen exchange data analysis

Hydrogen exchange rates were determined by fitting the decay in cross-peak volume *versus* time to the equation

$$I = A\exp(-k_{ex}t) + C$$

where I represents the volume of the cross-peak, A the amplitude of the exchange curve, k_{ex} is the observed rate of hydrogen exchange, t is the time expressed in minutes, and C is a constant, which takes into account the residual non-deuterated water and the threshold setting used in the intensity calculations. Data were fitted using the program Kaleidagraph (Abelbeck Software) on a Macintosh computer.

The intrinsic rate constant of exchange, k_{int}, for each amide proton at the different values of pH and temperature were calculated according to reported equations from model peptides (Bai *et al*., 1993), taking into account the activation enthalpies for PDLA and the temperature variation of the water ionization constant (Covington *et al*., 1966). Wild-type CI2 has 11 acidic residues, which titrate below pH 4.5 (Tan *et al*., 1995); hence, it was assumed that under our conditions all acidic residues are negatively charged.

Calculation of $\Delta\Delta G_{ex}$ for the mutant proteins

$\Delta\Delta G_{ex}$ was determined by direct comparison of the exchange rate constants of the mutant with those of wild-type at the same pH, using equation (6). Where the pH values of the wild-type and mutant samples were slightly different, however, $\Delta\Delta G_{ex}$ was calculated by comparison of the protection factors of wild-type and mutant proteins. The protection factor was determined using the following equation

$$P = \frac{k_{int}}{k_{ex}} \tag{7}$$

using the value of k_{int} calculated at the pH and temperature of the sample. $\Delta\Delta G_{ex}$ was calculated using

$$\Delta\Delta G_{ex} = -RT\ln\left(\frac{P_{ex}^{wt}}{P_{ex}^{m}}\right) \tag{8}$$

Solvent accessible surface areas

Solvent accessible surface areas were calculated from the crystal structure of wild-type (McPhalen & James, 1987) and pseudo-wild-type CI2 (Harpaz *et al*., 1994) using the algorithm of Lee & Richards (1971). The solvent probe radius was set to 1.4 Å.

Acknowledgements

J. L. N. was supported by E. C. Human Capital and Mobility fellowship. L. S. I. was supported by a Beit Memorial fellowship in Medical Research, and D. E. O. by a fellowship from the Danish Natural Science Research Council. We thank Dr J. Clarke and Dr S. Perrett for helpful discussions.

References

Bai, Y., Milne, J. S., Mayne, L. & Englander, S. W. (1993). Primary structure effects on peptide group hydrogen exchange. *Proteins: Struct. Funct. Genet.* **17**, 75–86.

Bai, Y., Milne, J. S., Mayne, L. & Englander, S. W. (1994). Protein stability parameters measured by hydrogen exchange. *Proteins: Struct. Funct. Genet.* **20**, 4–14.

Bax, A., Ikura, M., Kay, L. E., Torchia, D. A. & Tschudin, R. (1990). Comparison of different modes of two-dimensional reverse-correlation NMR for the study of proteins. *J. Magn. Reson.* **86**, 304–318.

Clarke, J. & Fersht, A. R. (1996). An evaluation of the use of hydrogen exchange at equilibrium to probe intermediates on the protein folding pathway. *Folding Design,* **1**, 243–254.

Clarke, J., Hounslow, A. M., Bycroft, M. & Fersht, A. R. (1993). Local breathing and global unfolding in hydrogen exchange of barnase and its relationship to protein folding pathways. *Proc. Natl Acad. Sci. USA,* **90**, 9837–9841.

Clore, G. M., Gronenborn, A. M., James, M. N. G., Kjær, M., McPhalen, C. A. & Poulsen, F. M. (1987a). Comparison of the solution structure and X-ray structure of barley serine proteinase inhibitor 2. *Protein Eng.* **1**, 313–318.

Clore, G. M., Gronenborn, A. M., Kjær, M. & Poulsen, F. M. (1987b). The determination of the three-dimensional structure of barley serine proteinase inhibitor 2 by nuclear magnetic resonance, distance geometry and restrained molecular dynamics. *Protein Eng.* **1**, 305–312.

Covington, A. K., Robinson, R. A. & Bates, R. G. (1966). The ionization constant of deuterium oxide from 5 to 50°C. *J. Phys. Chem.* **70**, 3820–3824.

Creighton, T. E. (1993). *Proteins,* 2nd edit., W. H. Freeman and Co, New York.

Delepierre, M., Dobson, C. M., Karplus, M., Poulsen, F. M., States, D. J. & Wedin, R. E. (1987). Electrostatic effects and hydrogen exchange behaviour in proteins. The pH dependence of exchange rates in lysozyme. *J. Mol. Biol.* **197**, 111–130.

elMasry, N. F. & Fersht, A. R. (1994). Mutational analysis of the N-capping box of the α-helix of chymotrypsin inhibitor 2. *Protein Eng.* **7**, 777–782.

Englander, S. W. & Kallenbach, N. R. (1984). Hydrogen exchange and structural dynamics of protein and nucleic acids. *Quart. Rev. Biophys.* **16**, 521–655.

Englander, S. W., Sosnick, T. R., Englander, J. J. & Mayne, L. (1996). Mechanisms and uses of hydrogen exchange. *Curr. Opin. Struct. Biol.* **6**, 18–23.

Fersht, A. R. (1995). Optimisation of rates of protein folding: the nucleation-condensation mechanism and its implications. *Proc. Natl Acad. Sci. USA,* **92**, 10869–10873.

Harpaz, Y., elMasry, N. F., Fersht, A. R. & Henrick, K. (1994). Direct observation of better hydration at the N-terminus of an α-helix with glycine rather than alanine as the N-cap residue. *Proc. Natl Acad. Sci. USA,* **91**, 311–315.

Hvidt, A. & Nielsen, S. O. (1966). Hydrogen exchange in proteins. *Advan. Protein Chem.* **21**, 187–386.

Itzhaki, L. S., Otzen, D. E. & Fersht, A. R. (1995). The structure of the transition state for folding of chymotrypsin inhibitor-2 analysed by protein engineering methods: evidence for a nucleation-

condensation mechanism for protein folding. *J. Mol. Biol.* **254**, 260–288.
Itzhaki, L. S., Neira, J. L. & Fersht, A. R. (1997). Hydrogen exchange in chymotrypsin inhibitor 2 probed by denaturants and temperature. *J. Mol. Biol.* **270**, 89–98.
Jackson, S. E. & Fersht, A. R. (1991). Folding of chymotrypsin inhibitor-2. 1. Evidence for a two-state transition. *Biochemistry,* **30**, 10428–10435.
Jackson, S. E., Moracci, M., elMasry, M., Johnson, C. M. & Fersht, A. R. (1993a). Effect of cavity creating mutations in the hydrophobic core of chymotrypsin inhibitor 2. *Biochemistry,* **32**, 11259–11269.
Jackson, S. E., elMasry, N. F. & Fersht, A. R. (1993b). Structure of the hydrophobic core in the transition state for folding chymotrypsin inhibitor-2: a critical test o the protein engineering method of analysis. *Biochemistry,* **32**, 11270–11278.
Jandu, S. K., Ray, S., Brooks, R. & Leatherbarrow, R. J. (1990). Role of arginine 67 in the stabilization of chymotrypsin inhibitor 2: examination of amide proton exchange rates and denaturation thermodynamics of an engineered protein. *Biochemistry,* **29**, 6264–6269.
Jeener, J., Meier, B., Backman, P. & Ernst, R. R. (1979). Investigation of exchange processes by two-dimensional NMR spectroscopy. *J. Chem. Phys.* **71**, 4546–4550.
Kim, K.-S., Fuchs, J. A. & Woodward, C. K. (1993). Hydrogen exchange identifies native-state motional domains important in protein folding. *Biochemistry,* **32**, 9600–9608.
Kjær, M., Ludvingsen, S., Sorensen, O. W., Denys, L. A., Kindler, J. & Poulsen, F. M. (1987). Sequence specific assignment of the proton nuclear magnetic resonance spectrum of barley serine proteinase inhibitor 2. *Carslberg Res. Commun.* **52**, 353–362.
Lee, B. K. & Richards, F. M. (1971). The interpretation of protein structures: estimation of static accessibility. *J. Mol. Biol.* **55**, 379–400.
Li, A. & Daggett, V. (1995). Investigation of the solution structure of chymotrypsin inhibitor 2 using molecular dynamics: comparison to X-Ray crystallographic and NMR data. *Protein Eng.* **8**, 117–1128.
Linderstrøm-Lang, K. U. (1955). Deuterium exchange between peptides and water. In Symposium on peptide chemistry. *Chem. Soc. Spec. Publ.* **2**, 1–20.
Lowry, T. M. & John, W. T. (1910). Studies of dynamic isomerism. XII. The equations for two consecutive unimolecular changes. *J. Chem. Soc. ,* **97**, 2634–2645.
Ludvigsen, S., Shen, H., Kjær, M., Madsen, J. C. & Poulsen, F. M. (1991). Refinement of the three-dimensional solution structure of barley serine proteinase inhibitor 2 and comparison with the structures in crystals. *J. Mol. Biol.* **222**, 621–635.
Marion, D. & Wüthrich, K. (1983). Application of phase-sensitive two-dimensional correlated spectroscopy (COSY) for measurements of ^{1}H-^{1}H spin-spin coupling constants in proteins. *Biochem. Biophys. Res. Commun.* **11**, 967–975.
McPhalen, C. A. & James, M. N. G. (1987). Crystal and molecular structure of the serine protease inhibitor (CI-2) from barley seeds. *Biochemistry,* **26**, 261–269.
Otzen, D. E., Itzhaki, L. S., elMasry, N. F., Jackson, S. E. & Fersht, A. R. (194). Structure of the transition state for the folding/unfolding of chymotrypsin inhibitor-2 and its implications for mechanisms of protein folding. *Proc. Natl Acad. Sci. USA,* **91**, 10422–10425.
Perrett, S., Clarke, J., Hounslow, A. M. & Fersht, A. R. (1995). Relationship between equilibrium amide proton exchange behaviour and the folding pathway of barnase. *Biochemistry,* **34**, 9288–9298.
Qian, H., Mayo, S. L. & Morton, A. (1994). Protein hydrogen exchange in denaturant: quantitative analysis by a two process model. *Biochemistry,* **33**, 8167–8171.
Roder, H., Wagner, G. & Wüthrich, K. (1985). Amide proton exchange in proteins by EX1 kinetics: studies of the basic pancreatic trypsin inhibitor at variable p^{2}H and temperature. *Biochemistry,* **24**, 7396–7407.
Skelton, N. J., Kördel, J., Akke, M. & Chazin, W. J. (1992). Nuclear magnetic resonance studies of the internal dynamics in apo, $(Cd^{2+})_1$ and $(Ca^{2+})_2$ calbindin D_{9k}. The rates of amide proton exchange with solvent. *J. Mol. Biol.* **227**, 1100–1117.
Swint-Kruise, L. & Robertson, A. D. (1996). Temperature and pH dependencies of hydrogen exchange and global stability for ovomucoid third domain. *Biochemistry,* **35**, 171–180.
Tan, Y.-J., Oliveberg, M., Davis, B. & Fersht, A. R. (1995). Perturbed pK_A-values in the denatured states of proteins. *J. Mol. Biol.* **254**, 980–992.
Van Greet, L. (1968). Calculation of the methanol and glycol nuclear magnetic resonance thermometers with a static thermistor probe. *Anal. Chem.* **40**, 2227–2229.
Wagner, G. (1980). A novel application of Nuclear Overhauser Enhancement (NOE) in proteins: analysis of correlated events in the exchange of internal labile protons. *Biochem. Biophys. Res. Commun.* **97**, 614–620.
Wang, A., Robertson, A. D. & Bolen, D. W. (1995). Effects of a naturally occurring osmolyte in the internal dynamics of Ribonuclease A. *Biochemistry,* **34**, 15096–15104.
Woodward, C. K. & Hilton, B. D. (1980). Hydrogen isotope exchange kinetics of single protons in bovine pancreatic trypsin inhibitor. *Biophys. J.* **32**, 561–575.
Wüthrich, K. (1986). *NMR of Proteins and Nucleic Acids,* John Wiley & Sons, Inc., New York.

Edited by J. Karn

(Received 23 December 1996; received in revised form 14 March 1997; accepted 11 April 1997)